Agricultural and Forest Meteorology 384 (2026) 111171

Contents lists available at ScienceDirect

Agricultural and Forest Meteorology

journal homepage: www.elsevier.com/locate/agrformet

Delta Blue Intensity chronologies from Siberian larch reveal robust summer temperature signals across northern Eurasia

Viktoria V. Agapova [a], Jan Esper [b,c], Alexander V. Kirdyanov [a,d], Ulf Büntgen [c,e,f], Natalia N. Koshurnikova [a], Anatoly S. Prokushkin [d], Alexey I. Kolmogorov [a,g], Alberto Arzac [a,e,*]

[a] Siberian Federal University, 79 Svobodnii, Krasnoyarsk 660041, Russia
[b] Department of Geography, Johannes Gutenberg University, Mainz 55128, Germany
[c] Global Change Research Institute (CzechGlobe), Czech Academy of Sciences, 603 00 Brno, Czech Republic
[d] V.N. Sukachev Institute of Forest SB RAS, Federal Research Center "Krasnoyarsk Science Center SB RAS", Krasnoyarsk 660036, Russia
[e] Department of Geography, University of Cambridge, Cambridge CB2 3EN, United Kingdom
[f] Department of Geography, Faculty of Science, Masaryk University, 613 00 Brno, Czech Republic
[g] Ammosov North-Eastern Federal University, Yakutsk 677027, Russia

ARTICLE INFO

Keywords:
Climate change
Tree-ring width
Blue intensity
Larix spp.
Taiga
Tundra

ABSTRACT

The boreal forests of northern Eurasia are experiencing accelerated warming. Understanding the climate sensitivity of its dominant tree species is essential for predicting changes in the global carbon cycle. Here, we present the first network of tree-ring width (TRW) and Blue Intensity (BI) chronologies spanning the Siberian boreal forest. Our network includes six larch forests representing three major species (*Larix sibirica* Ledeb., *Larix gmelinii* (Rupr.) Rupr., and *Larix cajanderi* Mayr.) ranging from the Ural Mountains in the west to the Sakha Republic in the east. For each site, we developed chronologies of TRW, earlywood BI (EWBI), latewood BI (LWBI), and delta BI (DBI). All parameters show positive correlations with summer temperatures from 1961 to 2020 CE. LWBI and DBI exhibit stronger and temporally more stable signals than TRW, particularly for June-July temperatures at the northernmost sites. The significant temperature signals suggest a species- and parameter-independent thermal constraint of Siberian larch growth. Our findings advocate DBI as a viable, cost-efficient surrogate for traditional wood density measurements that are typically used to reconstruct summer temperatures at high northern latitudes.

1. Introduction

Forests of northern Eurasia play an indispensable role in regulating ecosystem functions, including water cycle, soil stability, and climate change mitigation (Schaphoff et al., 2016). Having evolved under cold and highly variable conditions, these forests are particularly vulnerable to global warming (Gauthier et al., 2015), especially as regional temperature increases exceed the global average (IPCC, 2023; Rantanen et al., 2022). The genus *Larix* is among the most widespread tree genera in Russian boreal forests, covering ca. 35.6% of the country's forested area (Rosleshoz, 2024). Larches are well adapted to extreme cold and nutrient-poor soils (Abaimov, 2010), and are becoming increasingly dominant at northern and upper treelines, often forming monospecific stands in permafrost regions (Abaimov, 2010). Due to their wide distribution, longevity (Taynik et al., 2023), and ecological significance, *Larix* species are fundamental to boreal ecosystem functioning. Understanding the impact of climate change on *Larix* growth is therefore essential, given their contributions to ecosystem resilience, carbon balance, and biodiversity.

Dendrochronological studies have extensively documented the climate sensitivity of *Larix* species using diverse parameters, including tree-ring width (TRW; e.g., Esper et al., 2010; Hellmann et al. 2016; Vaganov et al., 1996), maximum latewood density (MXD; e.g., Briffa et al., 1998, 2001, 2004, 2013; Kirdyanov et al., 2007, 2008, 2024a), quantitative wood anatomy (QWA; e.g., Vaganov, 1996; Fonti et al., 2015) and stable isotopes (Churakova (Sidorova) et al., 2019, 2022, 2023; Kirdyanov et al., 2008; Sidorova et al., 2009, 2011). For instance, TRW and MXD in *Larix sibirica* Ledeb. show consistent positive

* Corresponding author.
E-mail address: aarzak@sfu-kras.ru (A. Arzac).

https://doi.org/10.1016/j.agrformet.2026.111171
Received 10 December 2025; Received in revised form 11 March 2026; Accepted 2 April 2026
Available online 12 April 2026

correlations with summer temperatures across Siberia (Arzac et al., 2025; Kirdyanov et al., 2007, 2024b; Kukarskih et al., 2018; Shiyatov, 1986). Similarly, the radial growth of *Larix gmelinii* (Rupr.) Rupr. in north-central Siberia is primarily limited by early summer temperatures (Vaganov et al., 1996; Kharuk et al., 2015), though responses remain site-specific even under permafrost conditions (Kirdyanov et al., 2013). Studies on *Larix cajanderi* Mayr. in eastern Siberia indicate a recent shift toward earlier growing seasons and a potential reduction in temperature limitation due to warming and earlier snowmelt (Arzac et al., 2019; Khotcinskaia et al., 2024; Kirdyanov et al., 2024c).

While MXD remains one of the most reliable dendroclimatic proxies for reconstructing summer temperature variability (Briffa et al., 2002; Büntgen et al., 2024; Esper et al., 2025; Chen et al., 2021; Schweingruber, 1988), a critical limitation is that most foundational MXD-based studies in northern Russia were conducted several decades ago (e.g., Briffa et al., 1995; Vaganov et al., 1996). Consequently, their calibration primarily reflects pre-1990s climatic conditions, preceding the period of intense, accelerated warming in the Arctic (Overland and Wang, 2020; Hantemirov et al., 2022; Rantanen et al., 2022). The rapid Arctic warming has led to a shortened snow cover duration, higher permafrost thaw, and increased frequency of summer heat waves (Biskaborn et al., 2019; Bonan, 2008; Kirdyanov et al., 2024c), directly affecting tree phenology (Kirdyanov et al., 2024b). Capturing these rapid and recent temperature fluctuations requires proxies with high temporal resolution and strong climatic sensitivity that are also cost-effective to measure over large spatial scales.

In this context, Blue Intensity (BI) has emerged as a promising proxy for temperature in high-latitude and high-elevation forests (Agapova et al., 2024; Arzac et al., 2025; Björklund et al., 2021; Cerrato et al., 2023; Reid and Wilson 2020; Semenyak and Dolgova, 2023; Vyukhina and Gurskaya, 2022; Wilson et al., 2017), complementing traditional proxies like TRW and MXD (Björklund et al., 2014; Frank and Nicolussi, 2020; Reid and Wilson, 2020; Rydval et al., 2014; Wang et al., 2020; Wilson et al., 2014). BI measures the inverted reflectance of blue light from wood surfaces using RGB digital image analysis (Björklund et al., 2024), with the blue channel capturing climate-sensitive information (McCarroll et al., 2002). Three key parameters are derived: earlywood blue intensity (EWBI), which reflects conditions during the early growing season; latewood blue intensity (LWBI), which responds to late growing season conditions (Cao et al., 2020); and delta blue intensity (DBI), calculated as the difference between EWBI and LWBI (Björklund et al., 2024). DBI was initially developed to address low-frequency biases in BI-based data (Björklund et al., 2014), and it has also proven to capture strong and valuable climate signals (Wilson et al., 2017; Agapova et al., 2024; Arzac et al., 2025).

However, a systematic, large-scale evaluation of BI across the major Siberian larch species is lacking. This study presents the first assessment of the temperature sensitivity of EWBI, LWBI, and DBI across the wide Siberian boreal forest. Our sampling design was developed to capture substantial environmental heterogeneity by collecting wood cores from diverse forest-tundra and taiga sites across a vast geographical region from the Urals to the Sakha Republic (~4100 km), thereby allowing to compare the potentially common climate signals from trees growing under contrasting site conditions. We analyze these parameters alongside TRW over the period 1961–2020, a window encompassing the recent era of intense anthropogenic warming. Our network includes six temperature-limited sites spanning the forest-tundra and taiga, and encompasses three ecologically distinct species: *L. sibirica, L. gmelinii*, and *L. cajanderi*. We hypothesize that *i)* LWBI and DBI will exhibit stronger and more stable correlations with summer temperatures than TRW across all species and sites, and *ii)* despite their ecological differences and the environmental heterogeneity represented by our sampling design, the three species will show a conserved common response to thermal constraints, while the specific timing and magnitude of the response will be modulated by local site conditions.

2. Methods

2.1. Description of study species

Siberian *Larix* show an eastward progression in cold adaptation. Western *L. sibirica* (60–120°E) grows on discontinuous permafrost under relatively mild conditions, with larger cones (10–50 mm) and needles (10–58 mm) (Abaimov, 2010; Bobrov, 1978). Central *L. gmelinii* (~110–127°E) tolerates continuous permafrost with intermediate morphology (cones: 5–35 mm; needles: 4–42 mm) (Abaimov, 2010). Northeastern *L. cajanderi* thrives in waterlogged permafrost with the smallest cones (9–28 mm) and shortest needles (6–33 mm) (Abaimov, 2010; Koropachinsky and Milutin, 2011). Species overlap occurs at 110–120°E (*L. sibirica/L. gmelinii*) and 120–127°E (*L. gmelinii/L. cajanderi*) (Bobrov, 1972), with genetic admixture challenging species boundaries (Semerikov and Lascoux, 1999; Zimmermann et al., 2019; Sheller et al., 2026).

2.2. Study area

The study area spans ~4100 km across northern Siberia, extending from the Ural Mountains in the west to the Sakha Republic in the east (59–70 °N and 59–147 °E). Six temperature-limited sites in the forest-tundra and mountain taiga vegetation zones were selected (Fig. 1A). These include three sites in the forest-tundra ecotone (northern treeline): Polar Urals (**PUR**), Igarka (**IGA**) and Chokurdakh (**CHO**); and three in the taiga: Northern Urals (**NUR**), and Suntar-Khayata (**SKH**) in the upper treeline, and Tura (TUR) in the northern taiga. Species composition reflects the ecological distribution of *Larix* across the region: *L. sibirica* dominates at **PUR, IGA**, and **NUR**; *L. gmelinii* at **TUR**, and *L. cajanderi* at **CHO** and **SKH**.

All sites are located within the sub-Arctic and Arctic climatic zones, characterized by extreme cold, continuous or discontinuous permafrost, and short growing seasons (<60 days; McBride and Douhovnikoff, 2012). Mean annual temperatures (1961–2020) range from −12.9 °C (**SKH**) to −0.2 °C (**NUR**), with June-August means varying from 8.0 °C (**CHO**) to 14.9 °C (**TUR**; Table 1). Annual precipitation totals range from 211 mm (**CHO**) to 850 mm (**NUR**), with over 33% occurring during the growing season (June-August; Fig. 1B). A significant warming trend was observed across all sites from 1961 to 2020 (Fig. S1). Mean annual temperatures increased at rates ranging from 0.25 °C per decade (**SKH**) to 0.54 °C per decade (**CHO**), with the most pronounced warming occurring in June (up to 0.90 °C per decade at **TUR**; Table S1). Monthly climate data were obtained from the nearest weather stations to each site at https://www.meteo.ru.

2.3. Sampling and chronology development

Increment cores (30–43 per site) were collected from dominant and co-dominant trees using a 5-mm borer during field campaigns in 2021 and 2022. In the laboratory, cores were processed to remove resins using 96% ethanol in a Soxhlet extractor over 72 hrs., followed by removal water-soluble substances at 80 °C for 48 hrs. (Cerrato et al., 2023). The cores were then air-dried and progressively polished up to 1200 grit. Polished core surfaces were scanned at 3200 dpi using an Epson Perfection V800 flatbed scanner interfaced with Silverfast software (LaserSoft Imaging, USA), with the scanner calibrated using an IT8 calibration target color card (Fuji, Japan), and shielded from external light (Rydval et al., 2014).

TRW, EWBI, and LWBI were measured on 185 cores using CooRecorder v9.3 (Cybis Elektronik & Data AB, Sweden). DBI was calculated by subtracting the ambient BI in the EWBI from the LWBI (DBI = LWBI – EWBI; Björklund et al., 2014, 2024). All TRW series were visually cross-dated, and statistically validated in COFECHA (Holmes, 1983). Non-climatic trends were removed from TRW, EWBI, LWBI, and DBI using a cubic smoothing spline, and chronologies were autoregressively

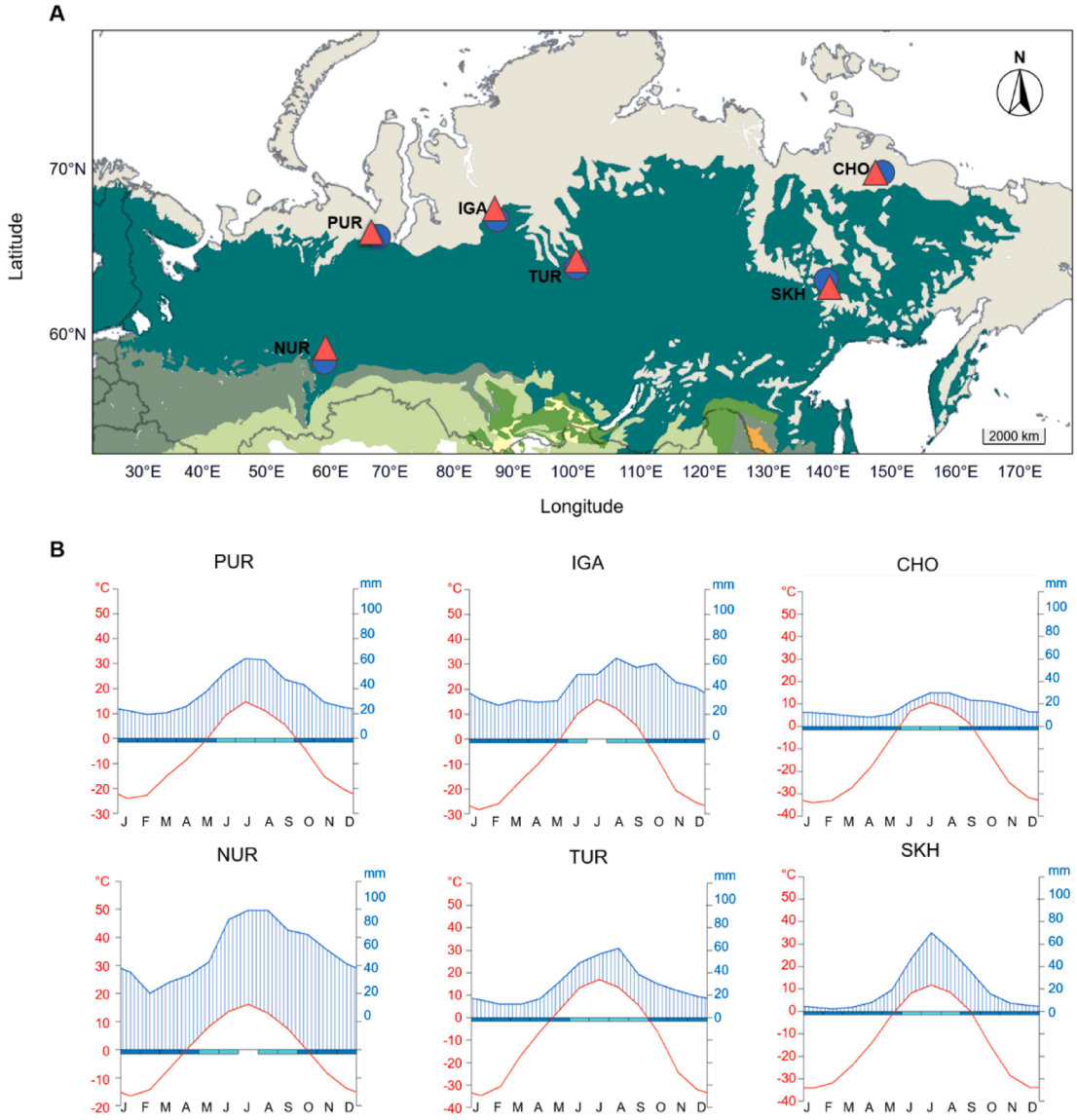

Fig. 1. (A) Distribution of sampling sites (circles) and their corresponding weather station (triangles). Shading indicates vegetation zones, tundra (light gray) and taiga (green). (B) Climate diagrams display monthly mean temperature (red line) and total precipitation (blue line) for the common period 1961–2020. **PUR** refers to Polar Urals, **IGA** to Igarka, **CHO** to Chokurdakh, **NUR** to Northern Urals, **TUR** to Tura, and **SKH** to Suntar-Khayata.

Table 1
Characterization of Siberian larch sites. **PUR** refers to Polar Urals, **IGA** to Igarka, **CHO** to Chokurdakh, **NUR** to Northern Urals, **TUR** to Tura, **SKH** to Suntar-Khayata, FT to forest-tundra, T to taiga, LASI to *L. sibirica*, LACA to *L. cajanderi*, and LAGM to *L. gmelinii*.

Parameter/site	PUR	IGA	CHO	NUR	TUR	SKH
Latitude	66°54′N	68°04′N	70°30′N	59°37′N	64°17′N	62°13′N
Longitude	65°45′E	86°44′E	147°11′E	59°15′E	100°13′E	139°31′E
Elevation (m a.s.l.)	125	77	71	750	492	1402
Vegetation zone	FT	FT	FT	T	T	T
Species	LASI	LASI	LACA	LASI	LAGM	LACA
Weather station	Salekhard	Igarka	Chokurdakh	Biser	Tura	Vostochnaya
Mean annual T (°C)	−5.68	−7.73	−13.38	−0.20	−8.51	−12.90
Mean June-July T (°C)	12.00	12.61	8.28	14.74	15.00	10.36
Mean June-August T (°C)	11.77	12.44	8.03	14.70	14.90	9.74
Annual P (mm)	450	527	211	850	367	274

modeled to remove autocorrelation and isolate annual climate signals. All dendrochronological analyses were performed using the "dplR" package (Bunn, 2008) in R (R Core Team, 2022). Chronology quality was assessed via expressed population signal (EPS > 0.85) over 30-year moving windows (Wigley et al., 1984; Briffa et al., 1995) and mean inter-series correlation (Rbar). In addition, unusually narrow tree rings were identified using extreme population mean values (Zchron; Jetschke et al., 2019; Qin et al., 2011). Specifically, a ring was classified as narrow when the z-score of its mean TRW index fell below a defined threshold of zTRW < −1. Finally, growth synchronism between

chronologies was evaluated using the Gleichläufigkeit (GLK > 60%; Eckstein and Bauch 1969; Lombardi et al., 2008) and correlation analysis.

2.4. Climate response analysis

Pearson's correlations were used to assess the relationship between residual chronologies (i.e., TRW, EWBI, LWBI, and DBI) and monthly climate variables (minimum, mean and maximum temperatures, and total precipitation) from September of the previous year to September of the current year over the 1961–2020 period. Climate data were linearly detrended prior to analysis to remove long-term trends (Ols et al., 2023). Cumulative effects of temperature and precipitation (i.e., June-July, June-August and June-September of the current year) were also evaluated. Daily moving correlations were used to identify the precise timing (day of the year, DOY) of maximal climate sensitivity at each site. The temporal stability of climate signals was assessed with 25-year running correlations (1-year interval) using the TreeClim package (Zang and Biondi, 2015) in R.

3. Results

3.1. Characteristics of chronologies

The residual TRW, LWBI, and DBI chronologies vary in length across sites, ranging from 210 years (**NUR**) to 533 years (**CHO**; Table 2 and Fig S2). TRW chronologies generally show the strongest statistical robustness, with all chronologies exceeding the EPS threshold of 0.85, except for EWBI at **PUR** and **CHO** (Table 2). Missing years are identified at all sites, reaching up to 91% of trees for the year 1967 at **NUR** (Table S2). Moreover, narrow rings occur simultaneously at three or more sites in several years (i.e., 1966, 1968, 1995, 1997, 2007, and 2020; Table S3 and Fig. S2). Collectively, these factors lead to extreme low values in several chronologies (particularly at **NUR** and **TUR**; Fig. S2). Therefore, the year 1967 was removed from further analysis at NUR due to the outlier value in the chronologies caused by its absence (and narrow ring formation when present). Although the sites are separated by large geographical distances (Table S4), statistically significant correlations exist among chronologies (Fig. 2 and Table S5). For *L. sibirica*, TRW shows significant inter-site correlations between **PUR** and **NUR** ($r = 0.32$; $p < 0.01$), and between **PUR** and **IGA** ($r = 0.45$; $p < 0.01$). LWBI correlations are particularly high between **TUR** and **IGA** (0.72; $p < 0.01$). The GLK index further confirms synchronicity, with TRW showing 63–73% agreement between **IGA, TUR**, and **PUR**, while LWBI reaches 71–81% for the same pairs. DBI shows similar pattern, with GLK values of 63–66% for **IGA-PUR** and **TUR-PUR**, respectively (Table S6).

3.2. Parameter-specific climate signals

All parameters correlate positively with summer temperatures, with the strongest responses to mean and maximum temperatures, particularly in LWBI and DBI (Fig. 3). June–July mean temperature emerges as the dominant climate driver across all site and parameters, albeit with variable strength.

TRW, LWBI and DBI in forest-tundra sites (**PUR, IGA**, and **CHO**) respond positively to June and July mean temperatures ($r > 0.38$; $p < 0.01$), though **CHO** TRW shows the weakest response in July. At **PUR** LWBI and DBI responses extend to August ($r > 0.33$; $p < 0.01$), while EWBI significantly correlates with June temperature ($r > 0.39$; $p < 0.01$) at **CHO**. At the taiga sites (**NUR, TUR**, and **SKH**) TRW, LWBI and DBI respond to June temperatures ($r > 0.40$; $p < 0.01$). EWBI only shows significant response at **TUR** (June, $r > 0.37$; $p < 0.01$). In general, the highest correlations across all sites are observed for aggregated June-July temperatures, although the strength of correlations varies across sites and parameters. The highest temperature signals are found at **CHO** and **PUR**, where DBI exhibits strong correlations ($r = 0.70$ and $r = 0.67$, $p < 0.001$, respectively). In contrast, **SKH** shows the weakest signal, with correlations ranging from $r = 0.40$ for LWBI to $r = 0.46$ for TRW ($p < 0.001$).

Precipitation signals remain weaker and site-specific. DBI correlates negatively with July precipitations at **NUR** ($r = -0.35$, $p < 0.01$), while TRW and LWBI at **PUR** respond to May and June-July precipitations ($r = -0.35$ to -0.36, $p < 0.001$). EWBI shows marginally positive effect of current September precipitation at **IGA** and previous September at **PUR**.

Daily moving correlations identify distinct windows of peak temperature sensitivity, primarily between DOY 150–200 (May 30th to July

Table 2
Characteristics of the tree-ring width (TRW), latewood blue intensity (LWBI), delta blue intensity (DBI), and earlywood blue intensity (EWBI) chronologies. **PUR** refers to Polar Urals, **IGA** to Igarka, **CHO** to Chokurdakh, **NUR** to Northern Urals, **SKH** to Suntar-Khayata, **TUR** to Tura, ms_x to mean sensitivity, Rbar to mean inter-series correlation, SNR to signal-to-noise ratio, and EPS expressed population signal. No trees EPS > 0.85 and year EPS > 0.85, represent the number of trees and the year in which EPS > 0.85 is reached, respectively.

	Site	Parameter	total No trees	start year	end year	ms_x	Rbar	SNR	EPS	No. trees EPS>0.85
Forest-tundra	PUR	TRW	26	1811	2020	0.41	0.65	48.46	0.98	4
		LWBI	25	1811	2020	0.08	0.42	17.72	0.95	4
		DBI	25	1811	2020	0.20	0.42	18.25	0.95	8
		EWBI	25	1811	2020	0.07	0.11	3.18	0.76	<0.85
	IGA	TRW	31	1687	2021	0.43	0.52	33.77	0.97	6
		LWBI	31	1687	2021	0.01	0.26	10.88	0.92	17
		DBI	31	1687	2021	0.22	0.30	13.41	0.93	14
		EWBI	31	1687	2021	0.09	0.14	5.098	0.84	<0.85
	CHO	TRW	43	1489	2021	0.44	0.50	42.34	0.98	8
		LWBI	42	1489	2021	0.14	0.34	21.21	0.96	12
		DBI	43	1489	2021	0.36	0.34	21.98	0.96	12
		EWBI	43	1489	2021	0.26	0.07	3.11	0.76	<0.85
Upper treeline	NUR	TRW	23	1816	2020	0.52	0.62	37.20	0.97	4
		LWBI	22	1816	2020	0.10	0.47	19.10	0.95	7
		DBI	22	1816	2020	0.22	0.45	18.26	0.95	7
		EWBI	22	1816	2020	0.09	0.21	5.66	0.85	18
	SKH	TRW	29	1623	2021	0.40	0.49	28.22	0.97	6
		LWBI	29	1623	2021	0.14	0.35	15.42	0.94	11
		DBI	29	1623	2021	0.26	0.38	17.87	0.95	10
		EWBI	29	1623	2021	0.14	0.17	5.86	0.85	28
Northern taiga	TUR	TRW	20	1779	2020	0.40	0.46	17.02	0.95	7
		LWBI	20	1787	2020	0.10	0.31	8.90	0.90	13
		DBI	20	1787	2020	0.24	0.23	7.91	0.89	15
		EWBI	20	1787	2020	0.18	0.20	4.95	0.83	<0.85

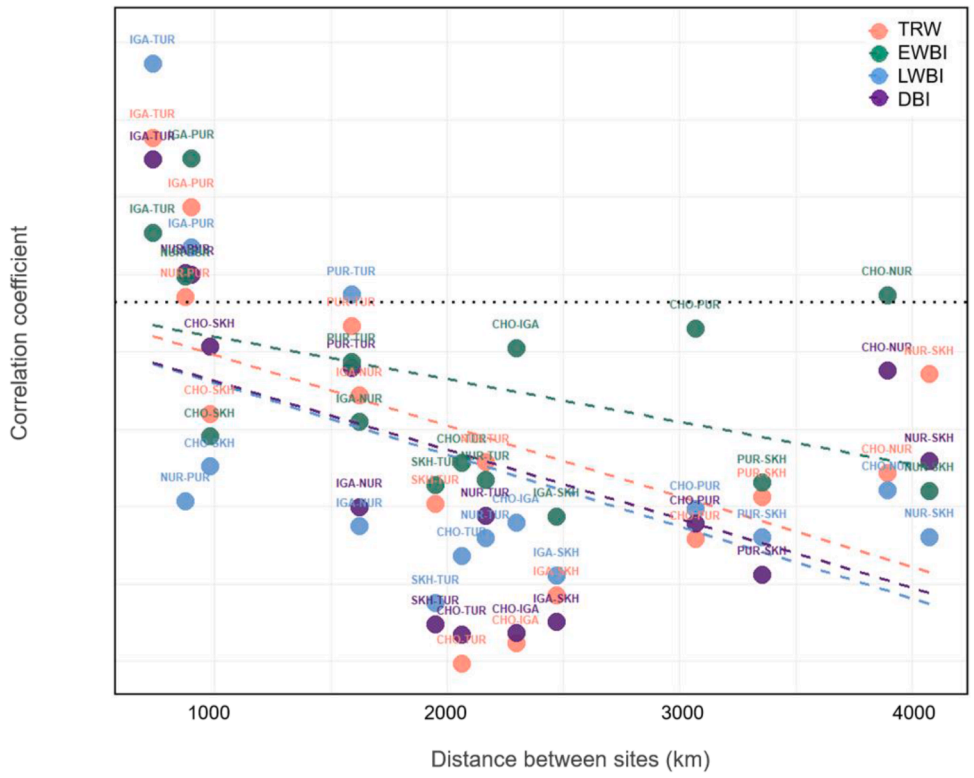

Fig. 2. Correlation between tree-ring width (TRW), earlywood blue intensity (EWBI), latewood blue intensity (LWBI), and delta blue intensity (DBI) indices among six larch sites over the common period 1961–2020. The x-axis represents the geographic distance between site pairs (in km), and the y-axis shows the Pearson correlation coefficient. The black dashed line indicates $p < 0.01$. **PUR** refers to Polar Urals, **IGA** to Igarka, **CHO** to Chokurdakh, **NUR** to Northern Urals, **TUR** to Tura, and **SKH** to Suntar-Khayata.

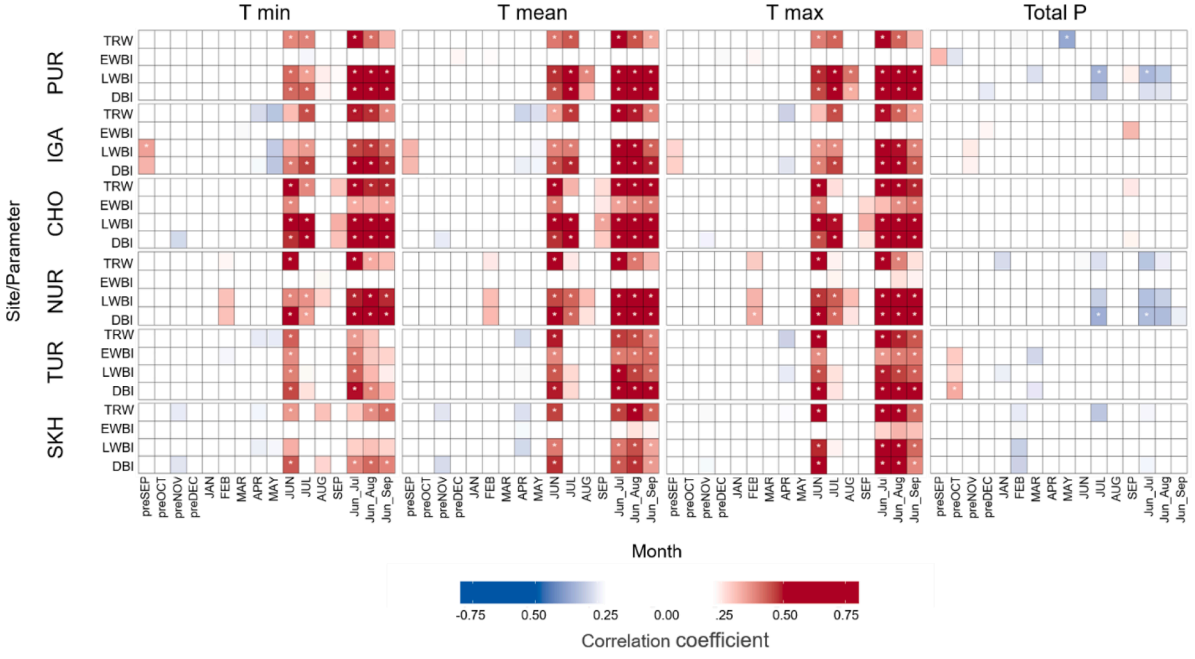

Fig. 3. Pearson correlations between tree-ring width (TRW), earlywood blue intensity (EWBI), latewood blue intensity (LWBI), and delta blue intensity (DBI) residual chronologies with minimum (T min), mean (T mean) and maximum (T max) monthly temperature and total monthly precipitation (Total P) over the 1961–2020 period. Correlations are calculated from the previous year September to current-year September and cumulative June-July, June-August and June-September of the current year. All colored cells are significant at $p < 0.05$. Asterisks indicate correlations at $p < 0.01$. **PUR** refers to Polar Urals, **IGA** to Igarka, **CHO** to Chokurdakh, **NUR** to Northern Urals, **TUR** to Tura, and **SKH** to Suntar-Khayata.

19th; Fig. S3 and Table S7). BI parameters at **IGA** and **CHO** show longer response durations (49-day window) than TRW (43 and 31 days, respectively). At **NUR**, the timing and duration of responses vary by the parameter, with LWBI responding earlier in DOY 118 (April 28th, over

an 89-day window), TRW responding in DOY 153 (Jun 2nd, over 44 days), while LWBI and DBI show a longer windows peaking around DOY 150–156 (May 30th-June 5th), spanning 72 and 79 days, respectively. At **SKH**, all parameters show a 30-day window centered in late May, with significant correlation ($r = 0.46$; $p < 0.001$). Temperature effects are consistently stronger at forest-tundra (northern treeline) sites than in taiga sites, particularly at **CHO**, where TRW and BI achieve the highest correlations ($r = 0.71$ and 0.70, respectively; $p < 0.001$). Across all sites, DBI outperformed LWBI in correlation strength.

3.3. Temporal stability of temperature responses

Yearly running correlations (1961–2020) reveal that LWBI and DBI maintain stable, high correlations ($p < 0.001$) with June-July temperatures, particularly at forest-tundra sites (**PUR, IGA**, and **CHO**; Fig. 4), while TRW sensitivity declines in most of the sites and EWBI shows weaker and most unstable signals. Among the forest-tundra sites, **PUR** shows the most stable signals overall, however, TRW declines from 1990 and EWBI shows an increasing trend since 1980, becoming marginally significant from 1996. At **IGA**, TRW, LWBI and DBI slightly decline from 1986 but remain significant, while EWBI increases since 1984 reaching correlation values similar to TRW by 2006. At **CHO**, TRW diverges from LWBI and DBI after 1986, with TRW showing consistently lower correlations. The sensitivity of LWBI and DBI also declines from 1992, while EWBI remains significant during the whole period.

At the taiga sites (**NUR, TUR**, and **SKH**), LWBI and DBI generally maintain strong correlations ($p < 0.001$) with June-July temperatures, while TRW shows higher temporal variability and EWBI remains the weakest and most unstable parameter. At **NUR**, TRW correlations increase steadily from 1961, peaking in 1985, and remaining consistently high thereafter. In contrast, LWBI and DBI rise after 1967, stabilize at high levels until 1990, and then show a slight decline while remaining significant. EWBI at **NUR** remains mostly low and non-significant throughout. At **TUR**, TRW exhibits moderate correlations until 1990, after which a marked decline occurs. LWBI and DBI maintain relatively high stability throughout most of the period. EWBI at **TUR**, initially near zero, reaches significant positive correlations after 1975 and remains stable thereafter. At **SKH**, TRW shows gradual upward trend from 1961 to 1990 before slightly declining. LWBI and DBI demonstrate persistently high and stable correlations, particularly after 1984. Correlations for EWBI at **SKH** remain unstable and generally low.

4. Discussion

Our study reveals a remarkable consistency in summer temperature sensitivity across three ecologically and geographically distinct Siberian larch species. Despite their geographical distribution and habitat heterogeneity, *L. sibirica, L. gmelinii*, and *L. cajanderi* exhibit parallel climate-growth responses, and synchronous occurrence of narrow rings, with DBI and LWBI consistently outperforming traditional TRW in temperature sensitivity. This uniformity in the response points to a conserved physiological adaptation to thermal constraints (e.g., Tei et al., 2014; Qi et al., 2023), likely linked to heat-dependent cambial activity and photosynthetic regulation (Zagirova, 2014; Vaganov et al., 2006; Silvestro et al., 2024).

The strongest temperature signals emerge in forest-tundra (northern treeline) sites, where LWBI and DBI show exceptional sensitivity to June-July temperatures. This heightened responsiveness reflects the marginal growth conditions of these high-latitude environments, where even minor temperature fluctuations during the short growing season significantly impact tree growth (Vaganov et al., 1996; Briffa et al., 2001; Knorre et al., 2006; Esper et al., 2010). Such sensitivity represents an adaptive strategy in which larches maximize resource accumulation during brief Arctic summers (Vaganov et al., 2006). In the taiga, where the growing season is relatively longer (Bryukhanova et al., 2013; Shishov et al., 2016), June temperatures remain a critical trigger for photosynthesis and earlywood formation. The observed general decline in TRW temperature sensitivity in recent decades may result from

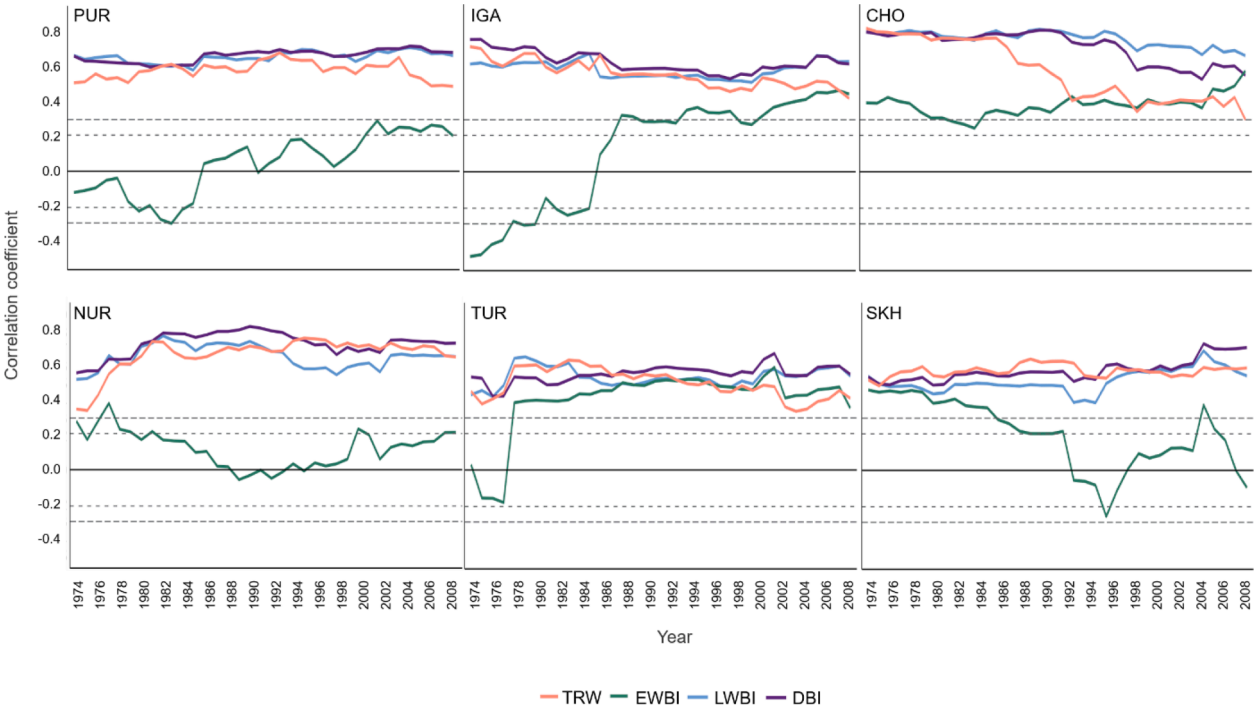

Fig. 4. Centered 25-year running correlations of tree-ring width (TRW in orange), early blue intensity (EWBI in green), latewood blue intensity (LWBI in blue) and delta blue intensity (DBI in light purple) residual chronologies against June-July mean temperatures over the 1961–2020 period. Dashed and dotted lines represent significant correlations at $p < 0.01$ and $p < 0.05$, respectively. **PUR** refers to Polar Urals, **IGA** to Igarka, **CHO** to Chokurdakh, **NUR** to Northern Urals, **TUR** to Tura, and **SKH** to Suntar-Khayata.

warming leading to more favorable growing conditions. Nevertheless, although this decline indicates a weakening of the strong thermal limitation, temperature control on growth remains evident across all sites. Moreover, despite the observed reduction in temperature sensitivity in TRW, the continued positive response of BI parameters to rising temperatures reflects an effective uptake of atmospheric CO_2 in Siberian boreal larch forests (Cuny et al., 2015; Silvestro et al., 2024; Li et al., 2025).

Although site heterogeneity exists in total annual precipitation and elevation, growing season length at all sites is primarily controlled by temperature, which govern the timing of snowmelt, soil thawing, constraining cambial activity and wood formation. Thus, while differences in elevation may introduce additional environmental complexity, temperature is the unifying limiting factor across the sites, as is evidenced by the synchronous occurrence of narrow rings. The biological mechanism for these patterns is rooted in xylogenesis (Rossi et al., 2007). When daytime temperatures exceed a critical threshold (~6 °C; Gurskaya, 2019), photosynthetic activity drives carbohydrate synthesis and cambial cell division (Deslauriers et al., 2008). This process promotes latewood cell wall thickening and lignification, which directly results in the darker latewood coloration (Briffa et al., 2002; Fonti et al., 2013), explaining the strong correlations between LWBI and DBI and summer temperatures. In contrast, the weak EWBI signal presents an important caveat. This likely results from a combination of biological factors such as the extremely narrow earlywood zones of 1–3 tracheid rows in these marginal environments (Vaganov et al., 2006), and technical limitations in reliably measuring such constrained anatomical features. This finding underscores the critical importance of parameter selection in high-latitude dendrochronology.

While most sites show the expected temperature-limited growth pattern (Fritts, 1976; Schweingruber, 1996; Vaganov et al., 1996), **PUR** and **NUR** exhibit negative correlations with precipitation. This likely reflects permafrost-mediated hydrological effects (Agapova et al., 2024), where early-season warming accelerates snowmelt (Kirdyanov et al., 2003; Vaganov et al., 1999), potentially leading to soil waterlogging (Kirdyanov et al., 2024c; Sugimoto et al., 2002) that suppresses radial growth (Manov, 2015). Excessive soil moisture can particularly impact latewood formation by reducing cambial activity (Gurskaya et al., 2012; Kirdyanov et al., 2013), thereby modulating LWBI and DBI values through altered latewood development.

The climate sensitivity of DBI closely mirrors that reported for MXD in previous studies across all sites, replicating its seasonal timing and temporal stability, robustly supporting its role as cost-effective alternative for high-resolution dendroclimatology (Agapova et al., 2024). At **CHO**, both proxies capture the extended summer signal (June-September) characteristic of this region (Kirdyanov et al., 2003, 2007), while at **SKH** they reflect the compressed growing season conditions through June-August responses (Kirdyanov et al., 2008). Regional variations are evident, with Central Siberian sites showing shorter optimal windows (June-August, July-August; Briffa et al., 2004). The superior performance of LWBI and DBI is visually and quantitatively confirmed by the direct comparison of residual chronologies with mean June–July temperatures (Figure S4). Across all sites, these parameters track interannual temperature fluctuations with remarkable fidelity, a synchrony most pronounced in forest-tundra environments. Moreover, the temperature sensitivity of both parameters remains quite stable during the recent warming period, except at **CHO**, where it tends to decline. This high temporal sensitivity solidifies their reliability as a surrogate of MXD for climate reconstruction across diverse Siberian environments. However, the BI methodology is not exempt from challenges. For instance, extremely narrow rings (Fig. S5) complicate measurements due to image resolution limitations (Björklund et al., 2019; Rydval et al., 2024), which, combined with a high frequency of missing rings, may contribute to the occurrence of extreme outliers in BI chronologies, such as those observed at **NUR** and **TUR** (Fig. S2).

The practical advantages of DBI, combined with the consistent patterns observed across three larch species, establishes its immense value for developing large-scale, high-resolution temperature reconstructions throughout northern Eurasia. This finding aligns with and extends the growing body of evidence supporting BI applications across the boreal forest, from North America to the Baltic region (Heeter et al., 2019; Janecka et al., 2020). Ultimately, the resilience of the DBI signal makes it an indispensable tool for monitoring the response of boreal forests to accelerating Arctic climate change.

5. Conclusions

This study establishes DBI as a superior temperature proxy across the vast Siberian larch forests, consistently outperforming traditional TRW in both signal strength and temporal stability. We found a striking uniformity in the temperature sensitivity of three ecologically distinct *Larix* species, underscoring a consistent response to thermal constraints governing cambial activity and photosynthesis. By analyzing the period 1961–2020, a window encompassing the recent intense Arctic warming, we demonstrate that DBI robustly captures the high-frequency temperature signal where traditional MXD chronologies are sparse. Consequently, our results validate DBI as a practical and cost-effective alternative to MXD, providing a much-needed proxy that reflects climatic conditions post-dating most of the MXD studies in the region. These findings provide an essential baseline for assessing boreal forest resilience and monitoring ecological responses to accelerating Arctic amplification. The reliable, stable temperature signal of DBI is particularly crucial for tracking the impacts of increasing heatwaves and pervasive permafrost degradation. Moving forward, expanding BI networks across underrepresented boreal regions and investigating precipitation-mediated modifications to these temperature responses will be essential to refine climate-growth models for our rapidly warming world.

CRediT authorship contribution statement

Viktoria V. Agapova: Writing – review & editing, Writing – original draft, Formal analysis, Data curation. **Jan Esper:** Writing – review & editing, Project administration, Funding acquisition, Conceptualization. **Alexander V. Kirdyanov:** Writing – review & editing, Methodology, Data curation, Conceptualization. **Ulf Büntgen:** Writing – review & editing, Funding acquisition, Conceptualization. **Natalia N. Koshurnikova:** Writing – review & editing, Data curation. **Anatoly S. Prokushkin:** Writing – review & editing, Data curation. **Alexey I. Kolmogorov:** Writing – review & editing, Data curation. **Alberto Arzac:** Writing – review & editing, Writing – original draft, Funding acquisition, Data curation, Conceptualization.

Declaration of competing interest

The authors declare the following financial interests/personal relationships which may be considered as potential competing interests: Alberto Arzac reports financial support was provided by Ministry of Science and Higher Education of the Russian Federation. Alberto Arzac reports financial support was provided by Russian Science Foundation. Alberto Arzac reports financial support was provided by Krasnoyarsk Regional Science Foundation. Jan Esper reports financial support was provided by European Research Council. If there are other authors, they declare that they have no known competing financial interests or personal relationships that could have appeared to influence the work reported in this paper.

Acknowledgments

This work was carried out with the support of the Ministry of Science and Higher Education of the Russian Federation [FSRZ-2020-0014, samplings], the Russian Science Foundation [project No 25-14-20060,

https://rscf.ru/project/25-14-20060/, measurements], and the Krasnoyarsk Regional Science Foundation. J.E. and U.B. received funding from the ERC project MONOSTAR [AdG 882727] and the ERC Synergy Grant [# 101118880; Synergy-Plague]. We thank V. Kukarskih, N. Devi. M. Tabakova and K. Akulinina for their support in field campaigns.

Supplementary materials

Supplementary material associated with this article can be found, in the online version, at doi:10.1016/j.agrformet.2026.111171.

Data availability

Data will be made available on request.

References

Abaimov, A.P., 2010. Geographical distribution and genetics of Siberian larch species. In: Osawa, A., Zyryanova, O.V., Matsuura, Y., Kajimoto, T., Wein, R.W. (Eds.), Permafrost Ecosystems: Siberian Larch Forests. Springer, Netherlands, pp. 41–58.

Agapova, V., Arzac, A., Kukarskih, V., Büntgen, U., Esper, J., Kirdyanov, A., 2024. Tree-ring blue intensity measurements from treeline sites in the Ural Mountains reveal summer temperature signal. Dendrochronologia 88, 126267. https://doi.org/10.1016/j.dendro.2024.126267.

Arzac, A., Popkova, M., Anarbekova, A., Olano, J.M., Gutiérrez, E., Nikolaev, A., Shishov, V., 2019. Increasing radial and latewood growth rates of *Larix cajanderi* Mayr. And *Pinus sylvestris* L. in the continuous permafrost zone in Central Yakutia (Russia). Ann. For. Sci. 76, 96. https://doi.org/10.1007/s13595-019-0881-1.

Arzac, A., Kirdyanov, A.V., Agapova, V.V., Kirdyanova, A.A., de Quijano, D.D., Bykov, N. I., Büntgen, U., 2025. Tree-ring width and blue intensity chronologies of three co-existing conifer species from the Russian Altai mountains reveal different climate signals. Dendrochronologia 93, 126382. https://doi.org/10.1016/j.dendro.2025.126382.

Biskaborn, B.K., Smith, S.L., Noetzli, J., et al., 2019. Permafrost is warming at a global scale. Nat. Commun. 10, 264. https://doi.org/10.1038/s41467-018-08240-4.

Björklund, J.A., Gunnarson, B.E., Seftigen, K., Esper, J., Linderholm, H.W., 2014. Blue intensity and density from northern Fennoscandian tree rings, exploring the potential to improve summer temperature reconstructions with earlywood information. Clim. Past 10, 877–885. https://doi.org/10.5194/cp-10-877-2014.

Björklund, J., von Arx, G., Nievergelt, D., Wilson, R., Van den Bulcke, J., Günther, B., Loader, N.J., Rydval, M., Fonti, P., Scharnweber, T., Andreu-Hayles, L., Büntgen, U., D'Arrigo, R., Davi, N., De Mil, T., Esper, J., Gärtner, H., Geary, J., Gunnarson, B.E., Hartl, C., Hevia, A., Song, H., Janecka, K., Kaczka, R.J., Kirdyanov, A.V., Kochbeck, M., Liu, Y., Meko, M., Mundo, I., Nicolussi, K., Oelkers, R., Pichler, T., Sánchez-Salguero, R., Schneider, L., Schweingruber, F., Timonen, M., Trouet, V., Van Acker, J., Verstege, A., Villalba, R., Wilmking, M., Frank, D., 2019. Scientific merits and analytical challenges of tree-ring densitometry. Rev. Geophys. 57, 1224–1264. https://doi.org/10.1029/2019RG000642.

Björklund, J., Fonti, M.V., Fonti, P., Van den Bulcke, J., von Arx, G., 2021. Cell wall dimensions reign supreme: cell wall composition is irrelevant for the temperature signal of latewood density/blue intensity in Scots pine. Dendrochronologia 65, 125785. https://doi.org/10.1016/j.dendro.2020.125785.

Björklund, J., Seftigen, K., Kaczka, R.J., Rydval, M., Wilson, R., 2024. A definition and standardised terminology for blue intensity from conifers. Dendrochronologia 85, 126200. https://doi.org/10.1016/j.dendro.2024.126200.

Bobrov, E.G. (1972). History and systematics of *Larix*. Nauka, Leningrad, 210 p. (in Russian).

Bobrov, E.G., 1978. Main Conifers in Forests of the Soviet Union. Nauka, Leningrad in Russian.

Bonan, G.B., 2008. Forests and climate change: forcings, feedbacks, and the climate benefits of forests. Science 320, 1444–1449. https://doi.org/10.1126/science.1155121.

Briffa, K.R., Jones, P.D., Schweingruber, F.H., Shiyatov, S.G., Cook, E.R., 1995. Unusual twentieth-century summer warmth in a 1,000-year temperature record from Siberia. Nature 376, 156–159. https://doi.org/10.1038/376156a0.

Briffa, K.R., Schweingruber, F.H., Jones, P.D., Osborn, T.J., Harris, I.C., Shiyatov, S.G., Vaganov, E.A., Grudd, H., 1998. Trees tell of past climates: but are they speaking less clearly today? Philos. Trans. R. Soc. B: Biol. Sci. 353 (1365), 65–73. https://doi.org/10.1098/rstb.1998.0191.

Briffa, K.R., Osborn, T.J., Schweingruber, F.H., Harris, I.C., Jones, P.D., Shiyatov, S.G., Vaganov, E.A., 2001. Low-frequency temperature variations from a northern tree-ring density network. J. Geophys. Res.: Atmos. 106 (D3), 2929–2941. https://doi.org/10.1029/2000JD900617.

Briffa, K.R., Osborn, T.J., Schweingruber, F.H., Jones, P.D., Shiyatov, S.G., Vaganov, E. A., 2002. Tree-ring width and density data around the Northern Hemisphere: part 1, local and regional climate signals. Holocene 12, 737–757. https://doi.org/10.1191/0959683602hl588rp.

Briffa, K.R., Osborn, T.J., Schweingruber, F.H., Jones, P.D., 2004. Large-scale temperature inferences from tree-rings: a review. Glob. Planet. Change 40 (1–2), 11–26. https://doi.org/10.1016/S0921-8181(03)00095-X.

Briffa, K.R., Melvin, T.M., Osborn, T.J., Hantemirov, R.M., Kirdyanov, A.V., Mazepa, V. S., Shiyatov, S.G., Esper, J., 2013. Reassessing the evidence for tree-growth and inferred temperature change during the Common Era in Yamalia, northwest Siberia. Quat. Sci. Rev. 72, 83–107. https://doi.org/10.1016/j.quascirev.2013.04.008.

Bryukhanova, M.V., Kirdyanov, A.V., Prokushkin, A.S., Silkin, P.P., 2013. Specific features of xylogenesis in Dahurian larch, *Larix gmelinii* (Rupr.) Rupr., growing on permafrost soils in Middle Siberia. Russ. J. Ecol. 44, 361–366. https://doi.org/10.1134/S1067413613050032.

Bunn, A.G., 2008. A dendrochronology program library in R (dplR). Dendrochronologia 26, 115–124. https://doi.org/10.1016/j.dendro.2008.01.002.

Büntgen, U., Reinig, F., Verstege, A., Piermattei, A., Kunz, M., Krusic, P., Slavin, P., Štěpánek, P., Torbenson, M., del Castillo, E.M., Arosio, T., Kirdyanov, A., Oppenheimer, C., Trnka, M., Palosse, A., Bebchuk, T., Camarero, J.J., Esper, J., 2024. Recent summer warming over the western Mediterranean region is unprecedented since medieval times. Glob. Planet. Change 232, 104336. https://doi.org/10.1016/j.gloplacha.2023.104336.

Cao, X., Fang, K., Chen, P., Zhang, P., Björklund, J., Pumijumnong, N., Guo, Z., 2020. Microdensitometric records from humid subtropical China show distinct climate signals in earlywood and latewood. Dendrochronologia 64, 125764. https://doi.org/10.1016/j.dendro.2020.125764.

Cerrato, R., Salvatore, M.C., Carrer, M., Brunetti, M., Baroni, C., 2023. Blue intensity of Swiss stone pine as a high-frequency temperature proxy in the Alps. Eur. J. For. Res. https://doi.org/10.1007/s10342-023-01566-9. Advance online publication.

Chen, F., Gagen, M.H., Zhang, H., Chen, Y., Fan, Z., Chen, F., 2021. Warm season temperature in the Qinling Mountains (north-central China) since 1740 CE recorded by tree-ring maximum latewood density of Shensi fir. Clim. Dyn. https://doi.org/10.1007/s00382-021-05827-4. Advance online publication.

Churakova (Sidorova), O.V., Fonti, M.V., Saurer, M., Guillet, S., Corona, C., Fonti, P., Myglan, V.S., Kirdyanov, A.V., Naumova, O.V., Ovchinnikov, D.V., Shashkin, A.V., Panyushkina, I.P., Büntgen, U., Hughes, M.K., Vaganov, E.A., Siegwolf, R.T.W., Stoffel, M., 2019. Siberian tree-ring and stable isotope proxies as indicators of temperature and moisture changes after major stratospheric volcanic eruptions. Clim. Past 15, 685–700. https://doi.org/10.5194/cp-15-685-2019.

Churakova (Sidorova), Fonti, M.V., Barinov, V.V., Zharkov, M.S., Taynik, A.V., Trushkina, T.V., Kirdyanov, A.V., Arzac, A., Saurer, M., 2022. Towards the third millennium changes in Siberian triple tree-ring stable isotopes. Forests 13. https://doi.org/10.3390/f13060934.

Churakova (Sidorova), O.V., Porter, T.J., Zharkov, M.S., Fonti, M.V., Barinov, V.V., Taynik, A.V., Kirdyanov, A.V., Knorre, A.A., Wegmann, M., Trushkina, T.V., Koshurnikova, N.N., Vaganov, E.A., Myglan, V.S., Siegwolf, R.T.W., Saurer, M., 2023. Climate impacts on tree-ring stable isotopes across the Northern hemispheric boreal zone. Sci. Total Environ. 870, 161644. https://doi.org/10.1016/j.scitotenv.2023.161644.

Cuny, H.E., Rathgeber, C.B.K., Frank, D., Fonti, P., Mäkinen, H., Prislan, P., Rossi, S., Martinez del Castillo, W., Campelo, F., Vavrčík, H., Camarero, J.J., Bryukhanova, M. V., Jyske, T., Gričar, J., Gryc, V., De Luis, M., Vieria, J., Čufar, K., Kirdyanov, A.V., Oberhuber, W., Treml, V., Huang, J.-G., Li, X., Swidrak, I., Deslauriers, A., Liang, E., Nöjd, P., Gruber, A., Nabiais, C., Morin, H., Krause, C., King, G., Fournier, M., 2015. Woody biomass production lags stem-girth increase by over one month in coniferous forests. Nat. Plants 1. https://doi.org/10.1038/nplants.2015.160.

Deslauriers, A., Rossi, S., Anfodillo, T., Saracino, A., 2008. Cambial phenology, wood formation and temperature thresholds in two contrasting years at high altitude in southern Italy. Tree Physiol. 28, 863–871. https://doi.org/10.1093/treephys/28.6.863.

Eckstein, D., Bauch, J., 1969. Beitrag zur rationalisierung eines dendrochronologischen verfahrens und zur analyse seiner Aussagesicherheit. Forstwiss. Cent. 88, 230–250. https://doi.org/10.1007/BF02741777.

Esper, J., Frank, D.C., Büntgen, U., Verstege, A., Hantemirov, R.M., Kirdyanov, A.V., 2010. Trends and uncertainties in Siberian indicators of 20th century warming. Glob. Change Biol. 16, 386–398. https://doi.org/10.1111/j.1365-2486.2009.01913.x.

Esper, J., Reinig, F., Torbenson, M., Martinez del Castillo, E., Kunz, M., Arzac, A., Carrer, M., Chen, F., Kadioglu, A.K., Kirdyanov, A.V., Tejedor, E., Trnka, M., Büntgen, U., 2025. Pan-alpine summer temperatures since 742 CE. Dendrochronologia 94, 126382.

Fonti, P., Bryukhanova, M.V., Myglan, V.S., Kirdyanov, A.V., Naumova, O.V., Vaganov, E.A., 2013. Temperature-induced responses of xylem structure of *larix sibirica* (Pinaceae) from the Russian Altay. Am. J. Bot. 100, 1332–1343. https://doi.org/10.3732/ajb.1200585.

Fonti, P., Tabakova, M.A., Kirdyanov, A.V., Bryukhanova, M.V., von Arx, G., 2015. Variability of ray anatomy of *Larix gmelinii* along a forest productivity gradient in Siberia. Trees 29, 1165–1175. https://doi.org/10.1007/s00468-015-1197-0.

Frank, T., Nicolussi, K., 2020. Testing different earlywood/latewood delimitations for the establishment of blue intensity data: a case study based on Alpine *Picea abies* samples. Dendrochronologia 64, 125775. https://doi.org/10.1016/j.dendro.2020.125775.

Fritts, H.C., 1976. Tree Rings and Climate. Academic Press.

Gauthier, S., Bernier, P., Kuuluvainen, T., Shvidenko, A.Z., Schepaschenko, D.G., 2015. Boreal forest health and global change. Science 349, 819–822. https://doi.org/10.1126/science.aaa9092.

Gurskaya, M., Hallinger, M., Singh, J., Agafonov, L., Wilmking, M., 2012. Temperature reconstruction in the Ob River valley based on ring widths of three coniferous tree species. Dendrochronologia 30, 302–309. https://doi.org/10.1016/j.dendro.2012.04.002.

Gurskaya, M.A., 2019. Effect of summer monthly temperatures on light tree ring formation in three larch species (*Larix*) in the northern forest–tundra of Siberia. Russ. J. Ecol. 50, 343–351. https://doi.org/10.1134/S1067413619040088.

Hantemirov, R.M., Corona, C., Guillet, S., Shiyatov, S.G., Stoffel, M., Osborn, T.J., Fonti, P., 2022. Current Siberian heating is unprecedented during the past seven millennia. Nat. Commun. 13, 4968. https://doi.org/10.1038/s41467-022-32629-x.

Heeter, K.J., Harley, G.L., Van De Gevel, S.L., White, P.B., 2019. Blue intensity as a temperature proxy in the eastern United States: a pilot study from a southern disjunct population of *Picea rubens* (Sarg.). Dendrochronologia 55, 105–109. https://doi.org/10.1016/j.dendro.2019.04.010.

Hellmann, L., Agafonov, L., Ljungqvist, F.C., Churakova, O., Düthorn, E., Esper, J., Hülsmann, L., Kirdyanov, A.V., Moiseev, P., Myglan, V.S., Nikolaev, A.N., Reinig, F., Schweingruber, F.H., Solomina, O., Tegel, W., Büntgen, U., 2016. Diverse growth trends and climate responses across Eurasia's boreal forest. Environ. Res. Lett. (11), 074021. https://doi.org/10.1088/1748-9326/11/7/074021.

Holmes, R.L., 1983. Computer-assisted quality control in tree-ring dating and measurement. Tree-Ring Bull. 43, 69–78.

Intergovernmental Panel on Climate Change (IPCC), 2023. Climate change 2023: synthesis report. Contribution of Working Groups I, II and III to the Sixth Assessment Report of the Intergovernmental Panel On Climate Change. IPCC. https://doi.org/10.59327/IPCC/AR6-9789291691647.

Janecka, K., Harvey, J.E., Trouillier, M., Kaczka, R.J., Metslaid, S., Metslaid, M., Buras, A., Wilmking, M., 2020. Higher winter-spring temperature and winter spring/summer moisture availability increase Scots pine growth on coastal dune microsites around the South Baltic Sea. Front. For. Glob. Change 3, 578912. https://doi.org/10.3389/ffgc.2020.578912.

Jetschke, G., van der Maaten, E., van der Maaten-Theunissen, M., 2019. Towards the extremes: a critical analysis of pointer year detection methods. Dendrochronologia 53, 55–62. https://doi.org/10.1016/j.dendro.2018.11.004.

Kharuk, V.I., Ranson, K.J., Im, S.T., Petrov, I.A., 2015. Climate-induced larch growth response within the central Siberian permafrost zone. Environ. Res. Lett. 10, 125009. https://doi.org/10.1088/1748-9326/10/12/125009.

Khotcinskaia, K.I., Sergeeva, O.V., Kirdyanov, A.V., Nikolaev, A.N., Akulinina, K.V., Koshurnikova, N.N., Arzac, A., 2024. Climatic response of radial growth of *Larix cajanderi* in Northern and Central Yakutia. Mosc. Univ. Biol. Sci. Bull. 79, 94–100. https://doi.org/10.3103/S0096392524700042.

Kirdyanov, A., Hughes, M., Vaganov, E., Schweingruber, F., Silkin, P., 2003. The importance of early summer temperature and date of snow melt for tree growth in the Siberian Subarctic. Trees 17, 61–69. https://doi.org/10.1007/s00468-002-0209-z.

Kirdyanov, A.V., Vaganov, E.A., Hughes, M.K., 2007. Separating the climatic signal from tree-ring width and maximum latewood density records. Trees 21, 37–44. https://doi.org/10.1007/s00468-006-0094-y.

Kirdyanov, A.V., Treydte, K.S., Nikolaev, A., Helle, G., Schleser, G.H., 2008. Climate signals in tree-ring width, density and δ^{13}c from larches in Eastern Siberia (Russia). Chem. Geol. 252, 31–41. https://doi.org/10.1016/j.chemgeo.2008.01.023.

Kirdyanov, A.V., Prokushkin, A.S., Tabakova, M.A., 2013. Tree-ring growth of Gmelin larch under contrasting local conditions in the north of Central Siberia. Dendrochronologia 31, 114–119. https://doi.org/10.1016/j.dendro.2012.10.003.

Kirdyanov, A.V., Arzac, A., Kirdyanova, A.A., Arosio, T., Ovchinnikov, D.V., Ganyushkin, D.A., Katjutin, P.N., Myglan, V.S., Nazarov, A.N., Slyusarenko, I.Y., Bebchuk, T., Büntgen, U., 2024a. Tree-ring chronologies from the upper treeline in the Russian Altai Mountains reveal strong and stable summer temperature signals. Forests 15, 1402. https://doi.org/10.3390/f15081402.

Kirdyanov, A.V., Kolmogorov, A.I., Kruse, S., Herzschuh, U., Arzac, A., Pestryakova, L.A., Nikolaev, A.N., Bebchuk, T., Büntgen, U., 2024b. Arctic amplification causes earlier onset of seasonal tree growth in northeastern Siberia. Environ. Res. Lett. 19, 114091. https://doi.org/10.1088/1748-9326/ad845f.

Kirdyanov, A.V., Saurer, M., Arzac, A., Knorre, A.A., Prokushkin, A.S., Churakova (Sidorova), O.V., Arosio, T., Bebchuk, T., Siegwolf, R., Büntgen, U., 2024c. Thawing permafrost can mitigate warming-induced drought stress in boreal forest trees. Sci. Total Environ. 912, 168858. https://doi.org/10.1016/j.scitotenv.2023.168858.

Knorre, A.A., Kirdyanov, A.V., Vaganov, E.A., 2006. Climatically induced inter-annual variations of productivity of aboveground biomass in forest-tundra and northern taiga of Central Siberia. Oecologia 147, 86–95. https://doi.org/10.1007/s00442-005-0249-3.

Koropachinsky, I.Yu., Milyutin, L.I, 2011. Botanical-geographical and forestry aspects of introgressive hybridization of Gmelin larch (*Larix gmelinii* (Rupr.) Rupr.) And Cajander larch (*L. cajanderi* Mair), 2, 225–238. Contemp. Probl. Ecol. 4, 167–177. https://doi.org/10.1134/S1995425511020081, 2011.

Kukarskih, V.V., Devi, N.M., Moiseev, P.A., Grigoriev, A.A., Bubnov, M.O., 2018. Latitudinal and temporal shifts in the radial growth-climate response of Siberian larch in the Polar Urals. J. Mt. Sci. 15, 722–729. https://doi.org/10.1007/s11629-017-4755-7.

Li, X., Silvestro, R., Liang, E., Mencuccini, M., Camarero, J.J., Rathgeber, C.B.K., Sylvain, J.D., Nabais, C., Giovannelli, A., Saracino, A., Saulino, L., Guerrieri, R., Gričar, J., Prislan, P., Peters, R.L., Čufar, K., Yang, B., Antonucci, S., Babushkina, E., Biondi, F., Campelo, F., Carrer, M., De Luis, M., Deslauriers, A., Drolet, G., Fajstavr, M., Fonti, M.V., Fonti, P., García-Valdés, R., Gruber, A., Gryc, V., Güney, A., Kašpar, J., Kirdyanov, A.V., Knorre, A.A., Lombardi, F., Mäkinen, H., Malik, R.A., Martinez del Castillo, E., Nöjd, P., Oberhuber, W., Ouimette, A.P., Shishov, V., Sukumar, R., Tognetti, R., Treml, V., Vavrčík, H., Vieira, J., Zeng, Q., Ziaco, E., Rossi, S., 2025. Warming increases the phenological mismatch between carbon sources and sinks in conifers. Nat. Clim. Change 15, 1363–1370. https://doi.org/10.1038/s41558-025-02474-z.

Lombardi, F., Cherubini, P., Lasserre, B., Tognetti, R., Marchetti, M., 2008. Tree rings used to assess time since death of deadwood of different decay classes in beech and silver fir forests in the central Apennines (Molise, Italy). Can. J. For. Res. 38, 821–833. https://doi.org/10.1139/X07-195.

Manov, A.V., 2015. Climatically induced variations in tree-ring chronologies of larch on the western macroslope of the Polar Urals. In: Current issues of biology and ecology: Proceedings of the XXII All-Russian youth scientific conference. Syktyvkar, pp. 36–41 in Russian.

McBride, J.R., Douhovnikoff, V., 2012. Characteristics of the urban forests in arctic and near-arctic cities. Urban For. Urban Green. 11, 113–119. https://doi.org/10.1016/j.ufug.2011.07.007.

McCarroll, D., Pettigrew, E., Luckman, A., Guibal, F., Edouard, J.L., 2002. Blue reflectance provides a surrogate for latewood density of high-latitude pine tree rings. Arct. Antarct. Alp. Res. 34, 450–453. https://doi.org/10.1080/15230430.2002.12003511.

Ols, C., Klesse, S., Girardin, M.P., Evans, M.E.K., DeRose, R.J., Trouet, V., 2023. Detrending climate data prior to climate–growth analyses in dendroecology: a common best practice? Dendrochronologia 79. https://doi.org/10.1016/j.dendro.2023.126094.

Overland, J.E., Wang, M., 2020. The 2020 Siberian heat wave. Int. J. Climatol. 41, E885–E890. https://doi.org/10.1002/joc.6850.

R Core Team, 2022. R: A Language and Environment For Statistical Computing. R Foundation for Statistical Computing. https://www.R-project.org/.

Qi, X., Cherubini, P., Treydte, K., Li, M.-H., Wu, Z., He, H.S., Du, H., Fang, K., Saurer, M., 2023. Growth responses to climate warming and their physiological mechanisms differ between mature and young larch trees in a boreal permafrost region. Agric. For. Meteorol. 343. https://doi.org/10.1016/j.agrformet.2023.109765.

Qin, C., Yang, B., Bräuning, A., Sonechkin, D.M., Huang, K., 2011. Regional extreme climate events on the northeastern Tibetan Plateau since AD 1450 inferred from tree rings. Glob. Planet. Change 75, 143–154. https://doi.org/10.1016/j.gloplacha.2010.10.013.

Rantanen, M., Karpechko, A.Y., Lipponen, A., Nordling, K., Hyvärinen, O., Ruosteenoja, K., Vihma, T., Laaksonen, A., 2022. The Arctic has warmed nearly four times faster than the globe since 1979. Commun. Earth Environ. 3, 168. https://doi.org/10.1038/s43247-022-00498-3.

Reid, E., Wilson, R., 2020. Delta blue intensity vs. maximum density: a case study using *Pinus uncinata* in the Pyrenees. Dendrochronologia 61, 125706. https://doi.org/10.1016/j.dendro.2020.125706.

Rosleshoz, 2024. Russian federal forestry agency. https://rosleshoz.gov.ru/news/2024-05-21/n10998 in Russian.

Rossi, S., Deslauriers, A., Anfodillo, T., Carraro, V., 2007. Evidence of threshold temperatures for xylogenesis in conifers at high altitudes. Oecologia 152, 1–12. https://doi.org/10.1007/s00442-006-0625-7.

Rydval, M., Larsson, L.Å., McGlynn, L., Gunnarson, B.E., Loader, N.J., Young, G.H.F., Wilson, R., 2014. Blue intensity for dendroclimatology: should we have the blues? Experiments from Scotland. Dendrochronologia 32, 191–204. https://doi.org/10.1016/j.dendro.2014.04.003.

Rydval, M., Björklund, J., von Arx, G., Begović, K., Lexa, M., Nogueira, J., Schurman, J. S., Jiang, Y., 2024. Ultra-high-resolution reflected-light imaging for dendrochronology. Dendrochronologia 83. https://doi.org/10.1016/j.dendro.2023.126160.

Schaphoff, S., Reyer, C.P.O., Schepaschenko, D., Gerten, D., Shvidenko, A., 2016. Tamm review: observed and projected climate change impacts on Russia's forests and its carbon balance. For. Ecol. Manag. 361, 432–444. https://doi.org/10.1016/j.foreco.2015.11.043.

Schweingruber, F.H., 1988. Tree rings: Basics and Applications of Dendrochronology. Kluwer Academic Publishers.

Schweingruber, F.H., Briffa, K.R., 1996. Tree-ring density networks for climate reconstruction. In: Jones, P.D., Bradley, R.S., Jouzel, J. (Eds.), Climatic Variations and Forcing Mechanisms of the Last 2000 Years. Springer, pp. 43–66. https://doi.org/10.1007/978-3-642-61113-1_3.

Semenyak, N., Dolgova, E., 2023. Dendroclimatic signals in the pine and spruce chronologies in the Solovetsky Archipelago. Dendrochronologia 77, 126029. https://doi.org/10.1016/j.dendro.2022.126029.

Semerikov, V.L., Lascoux, M., 1999. Genetic relationship among Eurasian and American *Larix* species based on allozymes. Heredity (Edinb) 83, 62–70. https://doi.org/10.1038/sj.hdy.6885310.

Sheller, M.A., Büntgen, U., Kirdyanov, A.V., Esper, J., Tabakova, M.A., György Tóth, E., Kukarskih, V.V., Kolmogorov, A.I., Ibe, A.A., Sukhikh, T.V., Bebchuk, T., Devi, N., Sergeeva, O.V., Agapova, V.V., Akulinina, K.V., Arzac, A., 2026. Genetic diversity suggests two rather than three larch (*Larix* spp.) species across Siberia. Perspect. Plant Ecol. Evol. Syst. 71, 125931. https://doi.org/10.1016/j.ppees.2026.125931.

Shishov, V.V., Tychkov, I.I., Popkova, M.I., Ilyin, V.A., Bryukhanova, M.V., Kirdyanov, A. V., 2016. VS-oscilloscope: a new tool to parameterize tree radial growth based on climate conditions. Dendrochronologia 39, 42–50. https://doi.org/10.1016/j.dendro.2015.10.001.

Sidorova, O.V., Siegwolf, R., Saurer, M., Shashkin, A.V., Knorre, A.A., Prokushkin, A.S., Vaganov, E.A., Kirdyanov, A.V., 2009. Do centennial tree-ring and stable isotope trends of *Larix gmelinii* (Rupr.) indicate increasing water shortage in the Siberian north? Oecologia 161, 825–835. https://doi.org/10.1007/s00442-009-1411-0.

Shiyatov, S.G., 1986. Dendrochronology of the Upper Timberline in the Urals. Nauka in Russian.

Sidorova, O.V., Siegwolf, R., Saurer, M., Naurzbaev, M., Shashkin, A.V., Vaganov, E.A., 2011. Spatial patterns of climatic changes in the Eurasian north reflected in Siberian larch tree-ring parameters and stable isotopes. Glob. Change Biol. 16, 1003–1018. https://doi.org/10.1111/j.1365-2486.2009.02008.x.

Silvestro, R., Mencuccini, M., García-Valdés, R., Antonucci, S., Arzac, A., Biondi, F., Rossi, S., 2024. Partial asynchrony of coniferous forest carbon sources and sinks at the intra-annual time scale. Nat. Commun. 15, 6169. https://doi.org/10.1038/s41467-024-49494-5.

Sugimoto, A., Yanagisawa, N., Naito, D., Fujita, N., Maximov, T.C., 2002. Importance of permafrost as a source of water for plants in east Siberian taiga. Ecol. Res. 17, 493–503. https://doi.org/10.1046/j.1440-1703.2002.00506.x.

Taynik, A.V., Myglan, V.S., Barinov, V.V., Oidupaa, O.C., Churakova, O.V., 2023. Ancient larch trees in the Tuva Republic, land of the oldest trees in Russia. J. Prot. Mt. Areas Res. Manag. 15 (2), 13–19. https://doi.org/10.1553/eco.mont-15-2s13.

Tei, S., Sugimoto, A., Yonenobu, H., Ohta, T., Maximov, T.F., 2014. Growth and physiological responses of larch trees to climate changes deduced from tree-ring widths and δ13C at two forest sites in eastern Siberia. Polar Sci. 8 (2), 183–195. https://doi.org/10.1016/j.polar.2013.12.002.

Vaganov, E.A., Shiyatov, S.G., Mazepa, V.S, 1996. Dendroclimatic Study in Ural-Siberian Subarctic. Nauka in Russian.

Vaganov, E.A., Hughes, M.K., Kirdyanov, A.V., Schweingruber, F.H., Silkin, P.P., 1999. Influence of snowfall and melt timing on tree growth in subarctic Eurasia. Nature 400, 149–151. https://doi.org/10.1038/22087.

Vaganov, E.A., Hughes, M.K., Shashkin, A.V., 2006. Growth Dynamics of Conifer Tree Rings: Images of Past and Future Environments. Springer.

Vyukhina, A.A., Gurskaya, M.A., 2022. Dendroclimatic potential of blue intensity-based chronologies of northern Fennoscandia Scots pine. J. Sib. Fed. Univ. - Biol. 15, 244–263. https://doi.org/10.17516/1997-1389-0385.

Wang, F., Arseneault, D., Boucher, É., Galipaud Gloaguen, G., Deharte, A., Yu, S., Troukechout, N., 2020. Temperature sensitivity of blue intensity, maximum latewood density, and ring width data of living black spruce trees in the eastern Canadian taiga. Dendrochronologia 64, 125771. https://doi.org/10.1016/j.dendro.2020.125771.

Wigley, T., Briffa, K., Jones, P., 1984. On the average value of correlated time series, with applications in dendroclimatology and hydrometeorology. J. Clim. Appl. Meteorol. 23, 201–213. https://doi.org/10.1175/1520-0450(1984)023<0201:OTAVOC>2.0.CO;2.

Wilson, R., Rao, R., Rydval, M., Wood, C., Larsson, L.Å., Luckman, B.H., 2014. Blue intensity for dendroclimatology: the BC blues: a case study from British Columbia, Canada. The Holocene 24, 1428–1438. https://doi.org/10.1177/0959683614544051.

Wilson, R., D'Arrigo, R., Andreu-Hayles, L., Oelkers, R., Wiles, G., Anchukaitis, K., Davi, N., 2017. Experiments based on blue intensity for reconstructing North Pacific temperatures along the Gulf of Alaska. Clim. Past 13, 1007–1022. https://doi.org/10.5194/cp-13-1007-2017.

Zagirova, S.V., 2014. Structure, pigment content and photosynthesis of Siberian larch needles in the Northern and subpolar Urals. For. Sci. 3, 3–10 in Russian.

Zang, C., Biondi, F., 2015. treeclim: an R package for the numerical calibration of proxy-climate relationships. Ecography 38, 431–436. https://doi.org/10.1111/ecog.01335.

Zimmermann, H.H., Harms, L., Epp, L.S., Bernhardt, N., Kruse, S., Stoof-Leichsenring, K. R., Petryakova, L.A., Wieczorek, M., Trense, D., Herzschuh, U., 2019. Chloroplast and mitochondrial genetic variation of larches at the Siberian tundra-taiga ecotone revealed by de novo assembly. PLoS One 14, e0216966. https://doi.org/10.1371/journal.pone.0216966.